# Simple surface treatment of conjugated polymers for enhanced cell adhesion using UV-Ozone

Megan M. Westwood, *[a,b] Peter A. Gilhooly-Finn,[a] Ryan P. Trueman,[a,c] Aisha Mumtaz,[a] Holly Gregory,[c] Joshua P. A. Daoud,[d] Avishek Dey,[a,e] Robert Palgrave,[a] Christopher A. R. Chapman,[d] James B. Phillips[c] and Bob C. Schroeder*[a]

[a] *Department of Chemistry, University College London, London, United Kingdom*

[b] *Department of Chemistry and Chemical Engineering, Chalmers University of Technology, Göteborg, Sweden.*

[c] *UCL Centre for Nerve Engineering, UCL School of Pharmacy, University College London, United Kingdom.*

[d] *Centre for Bioengineering, School of Engineering and Material Science, Queen Mary University of London, London, United Kingdom.*

[e] *London Centre for Nanotechnology, University College London, London, United Kingdom.*

**Abstract:** Aligning the material properties of organic semiconducting polymers to effectively interface with biological matter is critical for their use in bioelectronic devices. Synthetic modification and advanced processing techniques have typically been employed to promote cell adhesion and growth. In this study we apply UV-Ozone (UVO) treatment as a simple and accessible alternative for modifying pDPP3T films. Exposure to UVO increases polarity of the semiconductor surface, as confirmed by contact angle and XPS analysis. Surface treatment at and above the optimized time (t ≥ 30 s) consequently led to enhanced Schwann cell growth, with comparable behaviour to standard tissue culture plastic (TCP). Simultaneously, prolonged exposure begins to cause significant changes to the polymer's optical properties, with gradual photobleaching leading to the reduction in semiconducting behavior above 30 s. Leveraging the optimal biointerfacing properties of the UVO-treated pDPP3T, the validity of the technique in supporting cell viability and proliferation upon a semiconducting polymer was tested using electrical impedance spectroscopy. This work demonstrates the potential to more easily integrate conjugated polymers with biological environments, widening the opportunity to explore the interplay between ion diffusion and semiconductor electroactivity in the presence of biological cells.

## Introduction

Biological signals transmitted by living matter can be transduced into electronic pulses using organic bioelectronics.[1-3] Seamlessly connecting living tissue with conducting materials in this way poses great implications for the future of biosensing and tissue engineering.[4-6] Conjugated polymers (CPs) present an advantageous platform for developing these technologies as they demonstrate good biocompatibility, can be engineered into various form factors and can be tailored to a specific function through chemical design.[7-10] Progress in developing solid-state devices based on CPs such as field-effect transistors (OFETs) and photovoltaics (OPVs) has culminated in a rich understanding of their structure-property relationships. Consequently, their mechanical and electronic properties can be optimised through judicial chemical design and post processing techniques. However, for in vivo or in vitro implementation, the material requirements must be further extended to consider the biological properties. In particular, the ability of the material to support and facilitate cell growth is paramount to enabling these technologies.

Conducting polymers such as polypyrrole (PPy) and polyaniline (PANI) were amongst the first materials to constitute bioelectronic devices owing to their high biocompatibility and ease of synthesis.[11] However, low processability of the materials after synthesis limited their further development. More recently, synthetic efforts to ensure mixed ionic-electronic conduction focus on the introduction of hydrophilic motifs to CPs to allow for interaction with polar environments in organic electrochemical

transistors (OECTs). Successful examples of which are the use of side chains containing glycol functional groups or pendant polar moieties.[12-18] However, the intricacy in fine-tuning these materials often limits accessibility beyond the synthetic chemistry laboratory. Consequently, Poly(3,4-ethylenedixythiophene):poly(styrene sulphonate) (PEDOT:PSS) is the most renowned organic mixed ionic-electronic conductor (OMIEC) used in bioelectronics and cell culture studies due to simplicity in its production, in addition to having high processability and electronic performance. Though this renders PEDOT:PSS readily available to researchers across various disciplines, being limited to just one CP for all applications narrows the material space and opportunity to explore new technologies.

To improve cell adhesion and proliferation on polymer surfaces, many researchers modify the surface by altering mechanical properties and topography.[19-21] Yet, one of the most utilised and facile methods for facilitating cell adhesion to polymer surfaces involves altering the surface energy via exposure to plasma gas. A primary example of this is the use of tissue culture plastic (TCP) in the majority of cell culture laboratories, which mainly consists of polystyrene treated with plasma gas which drastically improves cell adhesion.[22] Depending on the gas used and time exposed, the surface can be modified to introduce new bonds such as COOH, COH, $NH_2$, SH.

Therefore, within this study we aimed to provide an alternative to the difficulties of problematic synthesis of OMIEC materials by applying surface functionalisation to a common CP to promote cell adhesion. Our choice of surface treatment was ultraviolet ozone (UVO) irradiation, a common and cost-effective laboratory technique used for cleaning surfaces. The CP, poly(2,2'-[(2,5-bis(2-hexyldecyl)-3,6-dioxo-2,3,5,6-tetrahydropyrrolo[3,4-*c*]pyrrole-1,4-diyl)dithiophene]-5,5'-diyl-alt-thiophen-2,5-diyl) (pDPP3T) was also chosen as it provides a high charge carrier mobility needed for electrical conduction.

To optimise the exposure time and understand the effect of functionalisation with UV-Ozone, pDPP3T thin films were exposed at increasing times of 1 – 1200 s. The optical properties of the thin films were then characterised using UV-Vis-NIR absorbance spectroscopy revealing a decrease in absorbance with increasing exposure time. Contact angle measurements and X-ray photoelectron spectroscopy (XPS) confirmed the introduction of oxygen containing functional groups, whilst atomic force microscopy (AFM) provided evidence for a smoothing of the surface with increased exposure time. Using electrical measurements and cell adhesion studies, the surface treatment time was optimised. To prove the suitability of our approach for cell interfacing, Schwann cells were successfully seeded onto the UVO treated pDPP3T thin films and electrical impedance spectroscopy (EIS) was used to measure cell count over time. We believe that the simple technique of UVO treatment, using readily available CP materials, will allow material scientists to electrically characterise cell culture without the need for intricate chemical modification or specialised processing techniques.

## Results and Discussion

### Effects of UV-Ozone on pDPP3T

Upon synthesizing pDPP3T, thin films were fabricated for characterization by spin coating from chlorobenzene solutions at 80 °C. The effect of UVO surface treatment on the semiconductor film properties was investigated by subjecting the films to varied exposure times of 0 s, 1 s, 5 s, 30 s, 60 s, 180 s, 600 s and 1200 s using an Ossila UV-Ozone cleaner. To assess changes to the polymer's optical properties after UVO exposure, UV-Vis-NIR spectroscopy was carried out and the resulting spectra are displayed in ***Figure 1a***. The pristine pDPP3T film exhibited two main absorption features, a π-π* band at 415 nm and the intramolecular charge transfer (ICT) band with $\lambda_{max}$ at 810 nm. After UVO exposure, a decrease in ICT absorbance relative to the π-π* band was observed, which took greater precedence with

increasing UV-Ozone exposure time (visualised in ***Supplementary Figure 2***). This in conjunction with blue shifting of π-π*, could indicate the breakdown of the conjugated polymer chains. It was found that beyond t = 600 s, the ICT band diminishes (as shown for t = 1200 s, ***Figure 1a***) and therefore further study was limited to UVO exposure times ≤ 600 s.

The surface energy ($\gamma_s$) of each film was calculated using the Fowkes model, by carrying out contact angle (θ) measurements using water and diiodomethane.[23] Utilizing the latter solvent, which exhibits negligible dispersive contribution to its surface tension ($\gamma_s^d$), allows determination of the polar ($\gamma_s^p$) and dispersive ($\gamma_s^d$) surface energy components. With increased UVO exposure, improved wetting of the film surface was observed through a large decrease in the water contact angle and an increase in total surface energy as shown in ***Figure 1b***. Upon extracting the separate dispersive and polar contributions (***Supplementary Table 1***), the increase in total surface energy was determined to be largely influenced by the latter.

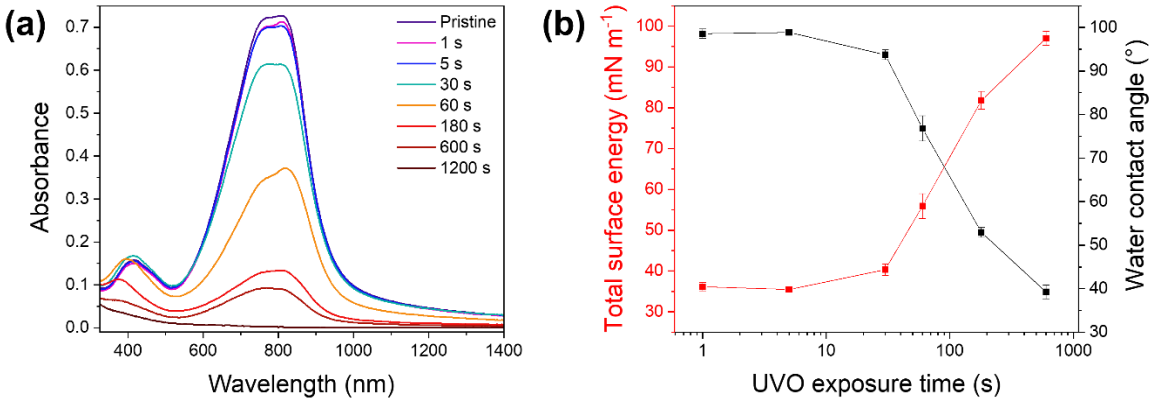


**Figure 1:** The effect of UVO surface treatment on pDPP3T films shown by (a) UV-Vis-NIR absorption spectra for films subjected to UV-Ozone surface treatment between 0 and 1200 s of exposure (b) total surface energy and the corresponding water contact angle at exposure times between 1 s and 600 s.

To gain insights into the contributions to the increase in surface energy, the chemical composition of the polymer surface after UVO exposure was studied using X-ray photoelectron spectroscopy (XPS). Regional data for C 1s, N 1s, O 1s and S 2p are given in **Figure 2** and full XPS survey between 0 and 600 eV in ***Supplementary Figure 3***. Complete elucidation of the decomposition mechanism and resulting structure is omitted due to being beyond the scope of this study. We instead focussed on qualitatively assessing the change in chemical environments due to surface treatment. The regional C 1s data is displayed in **Figure 2*a*** where the alternating single and double C-C bonds showed a peak at 284.4 eV in the pristine film, which slightly shifted to higher energy at 284.6 eV in the film treated for 600 s. This could be an indication of broken conjugation which would cause a shortening of the polymer chains, as corroborated by the reduction in the ICT band in UV-vis spectra. An additional band at lower energy (~285 eV) intensified after UVO exposure, corresponding to the formation of C-O and C=O functional groups after oxidation (typically reported between 285-289 eV).[24] The amide nitrogen in the DPP lactam ring exhibited a peak at ~400 eV in the N 1s spectra (**Figure 2*b***), which broadened with UVO exposure above 30 seconds. This could be explained by oxidation of the adjacent sidechain carbon.[25] The S 2p spectra for pristine pDPP3T displayed a single peak at 164.2 eV with unchanged relative intensity up to 60 seconds of UVO treatment (**Figure 2*d***). At this exposure time a second band at 168.6 eV associated with sulphur oxidation (S=O) emerged and increased in intensity with UVO exposure. This phenomenon is likely to contribute to the reduction in D-A character, as seen via UV-Vis absorbance, due to the

sulphur lone pair in thiophene no longer being available to donate into the ring. The surface elemental composition obtained from XPS clearly demonstrated oxidation of the CP films (***Supplementary Figure 4)***, resulting in the formation of more polar functional groups on the polymer surface, which provides further evidence for to the observed changes in polar and total surface energies discussed previously.

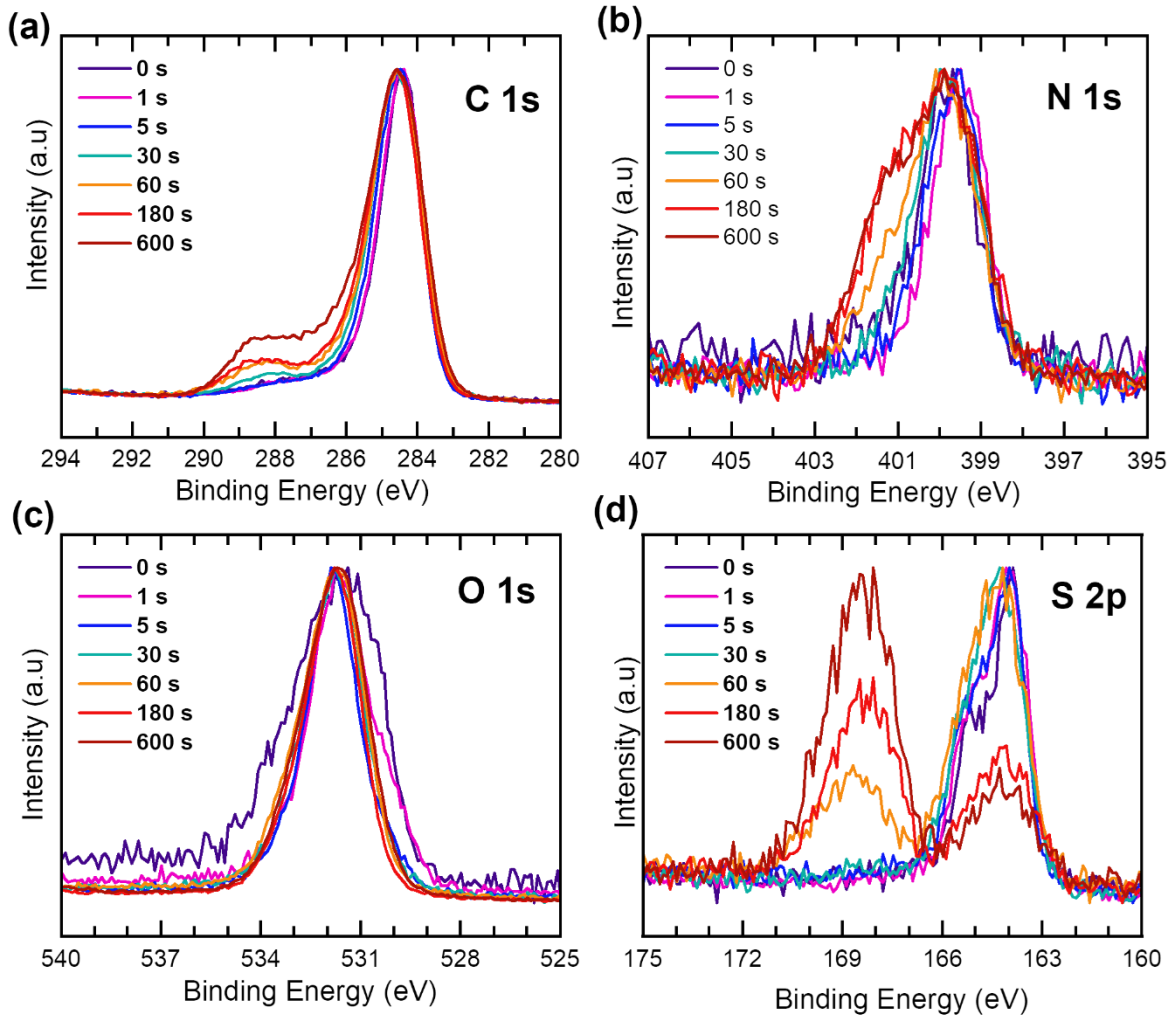


**Figure 2**: (a) C 1s, (b) N 1s, (c) O 1s and (d) S 2p XPS regional data obtained for pDPP3T films after varied UV-Ozone exposure times.

Atomic Force Microscopy (AFM) was used to gain insight into the topographic changes upon treating the CP films with UVO by capturing height images (***Figure 3a***). The pristine film exhibited a relatively flat, homogeneous surface with a roughness (arithmetical mean height, $R_a$) of 0.855 nm. The height images revealed smoothing of the polymer film surface which causes gradual reduction in surface roughness down to $R_a$ = 0.271 nm after 600 s (values listed in Supplementary Table 2). This can be visualized by plotting the displacement of the AFM tip along the xz axis (**Figure 3*b***) highlighting the increased surface homogeneity with prolonged UVO exposure time. After exposing the films for t ≥ 60 s, the formation of pin holes in the films became apparent in the height images, suggestive of the physical breakage of polymer chains which is concurrent with reduction in film thickness (***Supplementary Table 3***). It has been shown that surface roughness contributes to poor wettability in intrinsically hydrophobic surfaces ($\theta_{H2O}$ > 90°), whereas in intrinsically hydrophilic ($\theta_{H2O}$ < 90°) films wettability is enhanced with surface

roughness.[26] Consequently, the UVO smoothed film surfaces are likely to contribute to improved wettability in films treated for short times (t = 5 and 30 s), in addition to the increased surface energy introduced by partial oxidation of the surface.

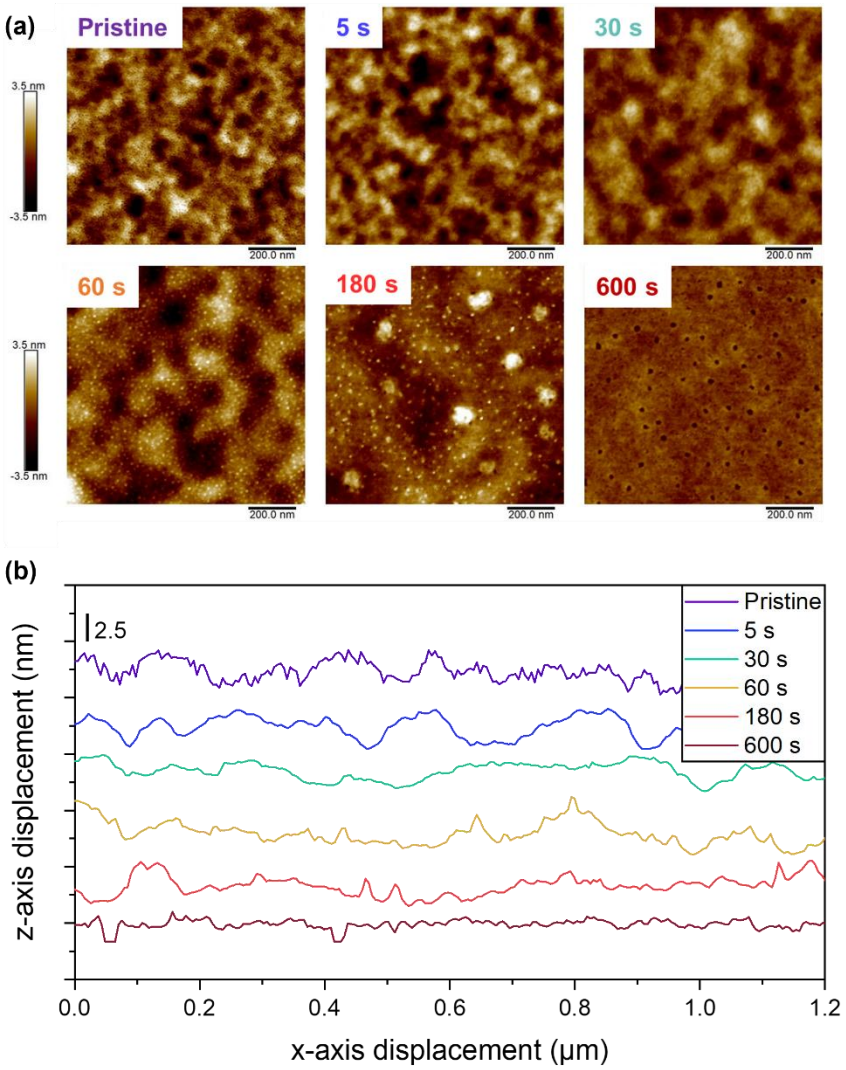


**Figure 3:** Surface morphology of pDPP3T films using AFM (a) height images of UV-Ozone treated pDPP3T films on glass substrates and (b) xz axial displacement of the AFM tip, taken from a cross section of the corresponding height image

**OFET device performance after UV-Ozone treatment**

To evaluate the impact of film modification on the electronic performance, bottom-gate bottom-contact (BGBC) organic field effect (OFET) devices were fabricated. Using field-effect measurements, the saturated hole mobilities were extracted from transfer curves using the gradient of $I_{ds}^{1/2}$ against $V_g$ (***Supplementary Figure 9***). The pristine pDPP3T film exhibited an average hole mobility ($\mu_h$) of $10.4 \times 10^{-2}$ $cm^2$ $V^{-1}$ $s^{-1}$; shown as the upper limit when comparing the effect of UVO treatment on OFET mobility in **Figure 4**. Upon short exposure of the films to ozone treatment (5 s and 30 s), the hole mobility is remarkably well maintained compared with the pristine film. However, with prolonged exposure times of 60 and 180 s, the mobility deteriorates by multiple orders of magnitude ($1.67 \times 10^{-4}$ and $4.92 \times 10^{-5}$ $cm^2$ $V^{-1}$ $s^{-1}$). Additionally, devices exposed to UVO for t > 30 s did not exhibit transistor-like characteristics

(inset, **Figure 4**), as seen by the inability to charge devices upon application of $V_g$. In agreement with the observed changes in chemical composition via XPS and reduction in the relative absorption of the ICT band in the UV-vis, this provides further evidence for a significant decrease in the effective conjugation of the pDPP3T due to oxidation of the polymer backbone. Yet, these results highlight the ability to retain desirable charge transport properties whilst simultaneously optimizing the surface properties through UVO treatment.

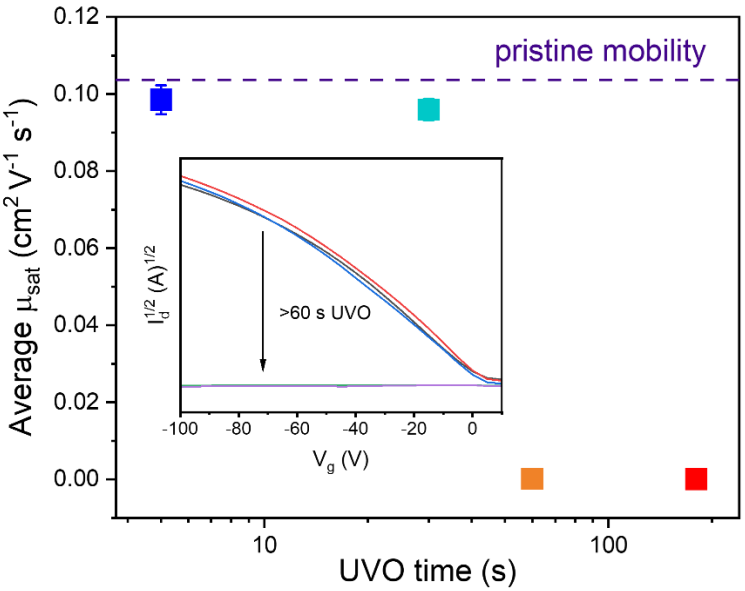


**Figure 4**: Comparison of the average saturated hole mobility ($\mu_{h,sat}$), extracted from transfer curves, averaged over 4 BGBC OFET devices. Devices consisted of 5 µm channel length, with the active layer exposed to varied UV-Ozone exposure times (5s, 30s, 60s and 180 s) compared against pristine (0s) pDPP3T (dashed line).

**Cell growth on pDPP3T films**

Once the impact of UVO treatment on the surface properties was understood, we sought to investigate how the enhancement in CP wettability translated to supporting and guiding interactions of living matter. We therefore seeded rat Schwann cells onto CP films treated with UVO and studied their growth over 48 hours. We utilised live cell phase contrast imaging to determine the number of cells at regular timepoints and assess cell morphology, in particular eccentricity. Statistical analysis of the cell count was carried out by fitting a mixed effects model followed by Dunnett's post-hoc test. Differences in cell eccentricity over time or between groups could not accurately be determined, owing to the tendency of the cells to cluster together (***Supplementary Figure 10***). As in vitro studies routinely employ tissue culture plastic (TCP) for cell culture, owing to its high surface energy and wettability, it was used as a positive control in this work.[27] Phase contrast micrographs displaying morphology and distribution of the cells on the treated films at 48 hours, shown in **Figure 5*a***, and **Figure 5*b***, show how cell count changes on the different materials over the duration of the study. For the pristine and 5 s exposed films a slow decline in the cell population number was observed after seeding. The lowest number of cells per field of view at 48 hours (66 ± 13) was observed in the absence of UV-Ozone treatment on pDPP3T, which incurred minor improvement after 5 s of UVO exposure (204 ± 62). However, we observed a substantial increase in the cell number compared to pristine film with UVO treatment t ≥ 30 seconds, as shown in ***Figure 5b***. Indeed, the number of cells per field was significantly greater than this control at all imaging timepoints from 6 hours onwards, amounting to cell counts of 974 ± 60 (30 s), 1051 ± 167 (60 s) and 1240 ± 104 (180 s) at 48 hours. This suggests that the observed changes in surface roughness

and surface energy contributes to the growth in the cell population on the treated polymer surfaces. Interestingly, the cell growth kinetics appear to improve at the same point where changes in the surface energy and UV-Vis characteristics of the pDPP3T films became apparent, following 30 seconds of UVO exposure.

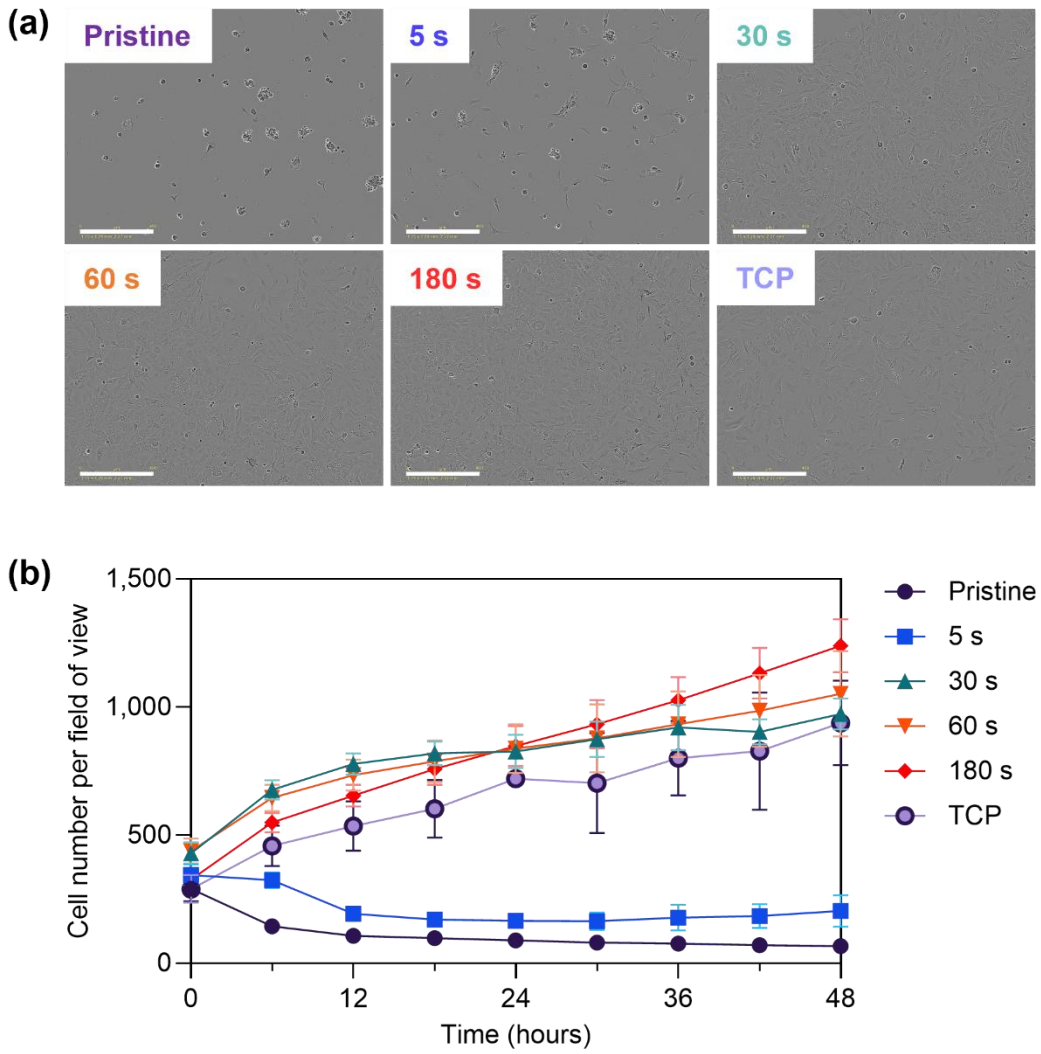


**Figure 5**: Schwann cell growth on UV-Ozone treated films and tissue culture plastic (TCP). (a) phase contrast micrographs at 48 h (scale bar: 400 µm) and (b) analysis of cell count over time. Mixed effects analysis showed statistically significant effects of time and group ($P < 0.0001$) with Dunnett's multiple comparisons test comparing each treatment group to pristine pDPP3T films indicating that the 5 s treatment group was not significantly different whereas all of the other groups were significantly different to pristine pDPP3T from 6 hours onwards.

**Electrical impedance of cell-seeded pDPP3T films**

Given that most bioelectronic device applications operate in ionic media, we sought to understand how the electronic properties were affected by the adherence of cells. Cells were seeded onto UV-Ozone treated pDPP3T films and impedance was monitored as a function of time. Electrical impedance spectroscopy (EIS) is a well utilised method for cell growth monitoring as impedance can be measured across a range of frequencies allowing for the electrical resistance and capacitance of cells to be extracted [28, 29]. The pDPP3T treated films were cast onto ITO coated glass and used as the working

electrode in a three-electrode electrochemical cell with platinum counter and Ag/AgCl reference electrodes. From our previous results, we found that t = 30 s exposure was suitable for promotion of cell growth while maintaining the electrical properties of the pDPP3T film. Therefore, the films were UV-Ozone treated using this optimised time before seeding with SCL4.1/F7 Schwann cells. As a control, 30 s UV-Ozone treated pDPP3T films were tested in cell culture media with no cells. EIS measurements were taken immediately before seeding (0 h), and at 6, 18, 24, 48, and 120 hours. The resulting impedance and phase plots for the films with and without Schwann cells are shown in ***Figure 6a*** and ***Figure 6b*** respectively. A clear reduction in low frequency (<100 Hz) impedance over time was observed in the pDPP3T films without cells (see ***Supplementary Figure 11*** for 100 Hz and 1 kHz measurements). The most pronounced impedance reduction due to cell growth was seen at 5 Hz and is highlighted in ***Figure 6c***.

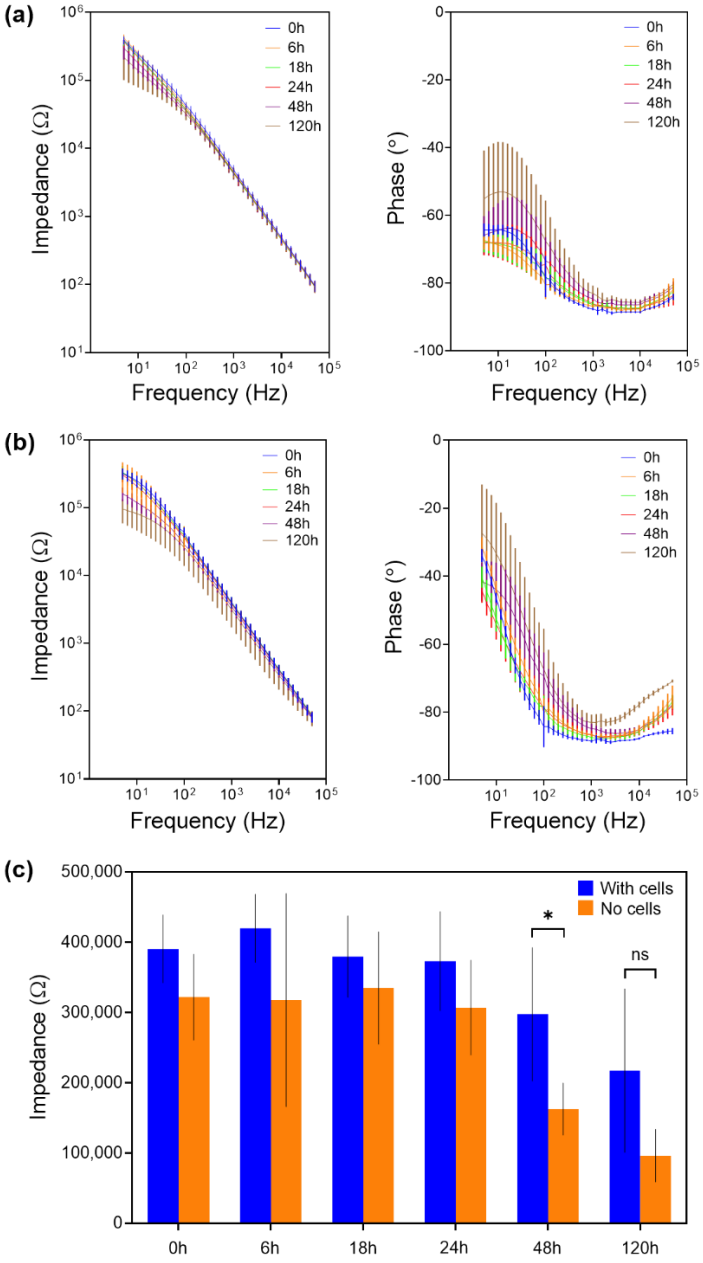


**Figure 6**: Electrical impedance spectra including real impedance and phase for pDPP3T films with Schwann cells (a) and without cells (b) at 0, 6, 18, 24, 48, and 120 hour time points, and (c) a specific comparison between real impedance values at 5 Hz between samples with and without cells. Sample size = 5 for all measurements. * - $p < 0.05$ using Welch's t-test between samples.

To correlate the impedance shift to cell growth, separate 30 s UV-Ozone treated pDPP3T films were seeded with SCL4.1/F7 Schwann cells and stained at each corresponding timepoint to visualise cell surface coverage and cell nuclei seen in ***Figure 7a***. Cell density was calculated by cell nucleus counting using ImageJ and is shown in ***Figure 7b***. The trend seen for these density calculations matched well with the previously observed cell counts shown in ***Figure 5a***. The ratio of pDPP3T film impedance with and without cells over time at a frequency of 5 Hz overlayed onto the cell density measurements (shown in ***Figure 7c)*** demonstrated strong similarity between the two datasets, suggesting that EIS increased with cell density on the film surface.

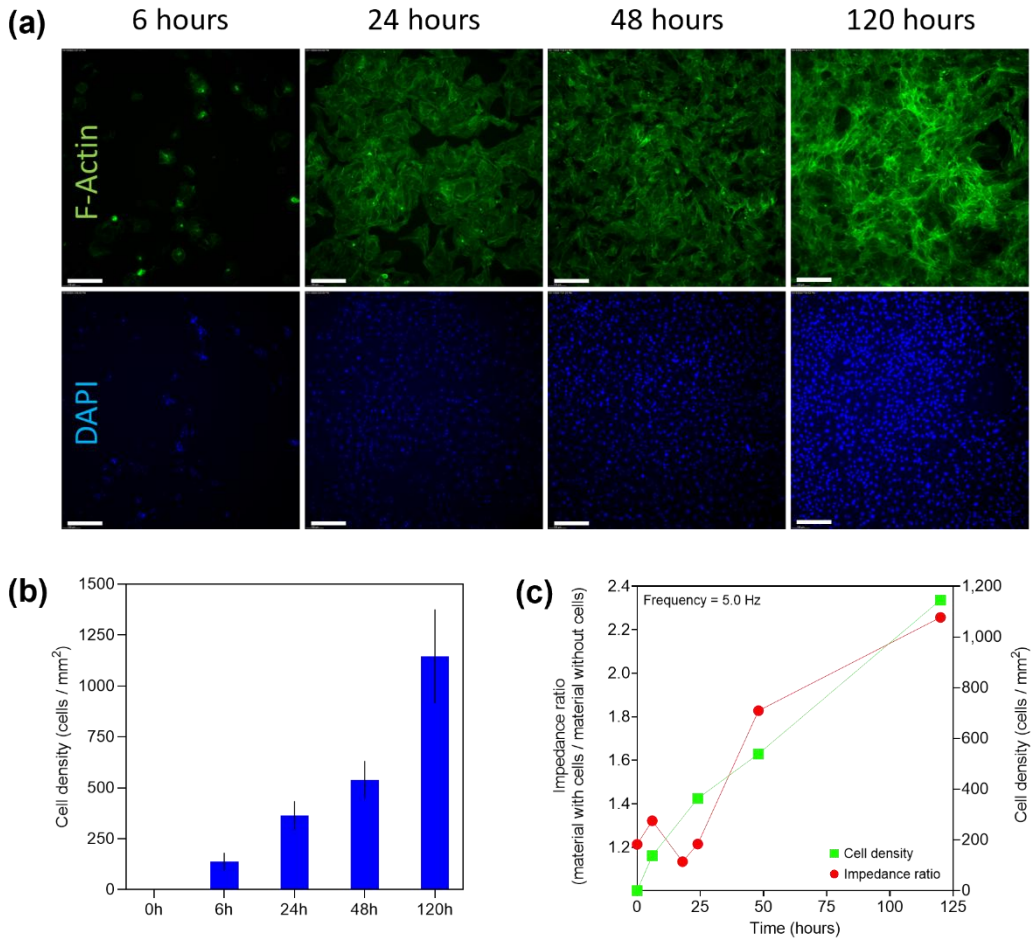


**Figure 7**: (a) Fluorescence micrographs (scale bar: 200 µm) showing SCL1.4/F7 Schwann cells cultured on 30 s UVO-treated pDPP3T films stained for F-Actin (phalloidin) and cell nucleus (DAPI). (b) SCL1.4/F7 Schwann cell density over time determined from DAPI stained images, and (c) a comparison between impedance ratio (with cells : without cells) and the cell density showing similar trends with increase impedance ratio as cell density increased. Sample size = 4 for all cell quantification.

---

In this study we observed a reduction in impedance in both UVO treated pDPP3T films over time, which could possibly be explained by diffusion of ionic media into the film whilst biasing, which is well known in CPs independent of their chemical composition.[30] By comparison of the datasets, it is observed that the presence of SCL4.1/F7 Schwann cells grown on the surface have an insulating effect, causing an increase in the lowering impedance, as is typical of bioimpedance measurements of materials with cell coverage.[28, 31] Yet, these results demonstrate the ability of UVO treated pDPP3T films to support interfacial cell growth whilst maintaining electroactivity. The intricacy in cell mediated processes at the electrode-electrolyte interface will vary with each selected matrix and CP substrate, the future study of

which is enabled by the UVO technique that provides a facile method to augment the biocompatibility of semiconducting polymers.[32]

## Conclusions

Herein we present an accessible and facile approach to improving the interaction of cells with an organic semiconducting (OSC) polymer film through UV-Ozone treatment. Variation of UVO exposure time was carried out to analyse the effect on pDPP3T films, which revealed an increase in the surface energy in combination with reduced surface roughness through contact angle and AFM measurements respectively. These properties culminated in an enhancement in Schwann cell growth on the surface with exposure times as low as t = 30 s. In addition to enhanced biocompatibility, retention of the optoelectronic properties in conjugated polymers is central to their application in bioelectronics. The effects of UVO exposure were monitored using UV-Vis absorption and field-effect measurements. These revealed that while the ICT band decreased relative to the π-π* band and the hole mobility declined with increasing exposure time, both changes were negligible for t ≤ 30 seconds.

Monitoring the optimized 30 s treated pDPP3T films using EIS in the presence of cells validated the use of UVO surface modification to sustain cellular interaction whilst under bias. As cell density on the surface increased over 120 h, the impedance ratio (relative to the non-seeded film) simultaneously increased. The use of UVO treatment to modulate cellular adhesion offers a valuable opportunity to deepen our understanding of the interplay between ionic diffusion and semiconductor electroactivity in the presence of cell culture media. By optimizing the exposure time for a given material, we believe this technique could be applied to a library of existing conjugated polymers, enabling in-operando studies of OSCs in biological environments.

## Author contributions

MMW, PGF, AM and BCS contributed to conception, design, data acquisition (UV-vis spectroscopy, UVO treatment, OFET, contact angle measurements, AFM) and interpretation, drafted, and critically revised the article. AD and RP contributed to data acquisition (XPS) and interpretation, drafted, and critically revised the article. RPT, HG and JBP contributed to data acquisition (Schwann cell work) and interpretation, drafted, and critically revised the article. JPAD and CARC contributed to data acquisition (EIS) and interpretation, drafted, and critically revised the article. All authors gave their final approval and agreed to be accountable for all aspects of the work.

## Conflicts of interest

There are no conflicts to declare.

## Data availability

Data for this article, including UV-vis absorption, OFET characterisation, contact angle data, EIS, XPS and phase contrast micrographs are available at UCL Research Data Repository at https://doi.org/10.5522/04/28220339.

## Acknowledgements

MMW, PGF and BCS would like to acknowledge funding from the UK Research and Innovation for Future Leaders Fellowship (MR/S031952/1 and MR/Y003802/1). AM is grateful for EPSRC PhD studentship

funding (EP/R513143/1 and EP/T517793/1). PGF and BCS would like to thank Dr Raphael Pfattner for lending his technical expertise with the field effect transistor measurements and the custom-built MATLAB OFET software, as well as Dr Robert Malinowski and Prof Giorgio Volpe for their assistance with the contact angle measurements. The X-ray photoelectron (XPS) data collection was performed at the EPSRC National Facility for XPS ("HarwellXPS"), operated by Cardiff University and UCL, under Contract No. PR16195. CARC and JPAD would like to acknowledge funding from Queen Mary University of London School of Engineering and Materials Science and The Royal Society [RGS\R2\242541] as well as Dr Maria Crespo Ribadeneyra for the use of her PalmSens4 potentiostat.

## References

1. D. T. Simon, E. O. Gabrielsson, K. Tybrandt and M. Berggren, *Chemical Reviews*, 2016, **116**, 13009-13041.
2. C. Pitsalidis, A. M. Pappa, A. J. Boys, Y. Fu, C. M. Moysidou, D. van Niekerk, J. Saez, A. Savva, D. Iandolo and R. M. Owens, *Chem Rev*, 2022, **122**, 4700-4790.
3. W. Wang, Y. Pan, Y. Shui, T. Hasan, I. M. Lei, S. G. S. Ka, T. Savin, S. Velasco-Bosom, Y. Cao, S. B. P. McLaren, Y. Cao, F. Xiong, G. G. Malliaras and Y. Y. S. Huang, *Nature Electronics*, 2024, **7**, 586-597.
4. S. G. Higgins, A. Lo Fiego, I. Patrick, A. Creamer and M. M. Stevens, *Advanced Materials Technologies*, 2020, **5**, 2000384.
5. R. P. Trueman, A. S. Ahlawat and J. B. Phillips, *Tissue Engineering Part B: Reviews*, 2022, **28**, 1137-1150.
6. N. Li, Y. Li, Z. Cheng, Y. Liu, Y. Dai, S. Kang, S. Li, N. Shan, S. Wai, A. Ziaja, Y. Wang, J. Strzalka, W. Liu, C. Zhang, X. Gu, J. A. Hubbell, B. Tian and S. Wang, *Science*, 2023, **381**, 686-693.
7. S. Inal, J. Rivnay, A. O. Suiu, G. G. Malliaras and I. McCulloch, *Acc Chem Res*, 2018, **51**, 1368-1376.
8. J. Tropp and J. Rivnay, *Journal of Materials Chemistry C*, 2021, **9**, 13543-13556.
9. D. Ohayon, D. Renn, S. Wustoni, K. Guo, V. Druet, A. Hama, X. Chen, I. P. Maria, S. Singh, S. Griggs, B. C. Schroeder, M. Rueping, I. McCulloch and S. Inal, *ACS Applied Materials & Interfaces*, 2023, **15**, 9726-9739.
10. C. J. Kousseff, S. Wustoni, R. K. S. Silva, A. Lifer, A. Savva, G. L. Frey, S. Inal and C. B. Nielsen, *Advanced Science*, 2024, **11**, 2308281.
11. R. Balint, N. J. Cassidy and S. H. Cartmell, *Acta Biomaterialia*, 2014, **10**, 2341-2353.
12. G. Oyman, C. Geyik, R. Ayranci, M. Ak, D. Odaci Demirkol, S. Timur and H. Coskunol, *RSC Advances*, 2014, **4**, 53411-53418.
13. A. Giovannitti, D.-T. Sbircea, S. Inal, C. B. Nielsen, E. Bandiello, D. A. Hanifi, M. Sessolo, G. G. Malliaras, I. McCulloch and J. Rivnay, *Proceedings of the National Academy of Sciences*, 2016, **113**, 12017-12022.
14. W. Du, D. Ohayon, C. Combe, L. Mottier, I. P. Maria, R. S. Ashraf, H. Fiumelli, S. Inal and I. McCulloch, *Chemistry of Materials*, 2018, **30**, 6164-6172.
15. A. Giovannitti, I. P. Maria, D. Hanifi, M. J. Donahue, D. Bryant, K. J. Barth, B. E. Makdah, A. Savva, D. Moia, M. Zetek, P. R. F. Barnes, O. G. Reid, S. Inal, G. Rumbles, G. G. Malliaras, J. Nelson, J. Rivnay and I. McCulloch, *Chemistry of Materials*, 2018, **30**, 2945-2953.
16. Y. Wang, S. Wustoni, J. Surgailis, Y. Zhong, A. Koklu and S. Inal, *Nature Reviews Materials*, 2024, **9**, 249-265.
17. H. Kim, Y. Won, H. W. Song, Y. Kwon, M. Jun and J. H. Oh, *Adv Sci (Weinh)*, 2024, **11**, e2306191.
18. S. Buchmann, P. Stoop, K. Roekevisch, S. Jain, R. Kroon, C. Müller, M. M. Hamedi, E. Zeglio and A. Herland, *ACS Applied Materials & Interfaces*, 2024, **16**, 54292-54303.
19. S. Cai, C. Wu, W. Yang, W. Liang, H. Yu and L. Liu, *Nanotechnology Reviews*, 2020, **9**, 971-989.
20. S. M. A. Mokhtar, A. L. K. Derrick-Roberts, D. R. Evans and X. L. Strudwick, *ACS Appl Bio Mater*, 2023, **6**, 4662-4671.
21. R. P. Trueman, P. G. Finn, M. M. Westwood, A. Dey, R. Palgrave, A. Tabor, J. B. Phillips and B. C. Schroeder, *Journal of Materials Chemistry C*, 2023, **11**, 6943-6950.
22. M. J. Lerman, J. Lembong, S. Muramoto, G. Gillen and J. P. Fisher, *Tissue Eng Part B Rev*, 2018, **24**, 359-372.
23. F. M. Fowkes, *Industrial & Engineering Chemistry*, 1964, **56**, 40-52.
24. D. Briggs and G. Beamson, *Analytical Chemistry*, 1992, **64**, 1729-1736.
25. M. A. Anderson, A. Hamstra, B. W. Larson and E. L. Ratcliff, *Journal of Materials Chemistry A*, 2023, **11**, 17858-17871.
26. T. Darmanin and F. Guittard, *Progress in Polymer Science*, 2014, **39**, 656-682.
27. E. M. Harnett, J. Alderman and T. Wood, *Colloids and Surfaces B: Biointerfaces*, 2007, **55**, 90-97.
28. Q. Hassan, S. Ahmadi and K. Kerman, *Micromachines (Basel)*, 2020, **11**.
29. C. Pitsalidis, D. van Niekerk, C. M. Moysidou, A. J. Boys, A. Withers, R. Vallet and R. M. Owens, *Sci Adv*, 2022, **8**, eabo4761.
30. A. A. Szumska, I. P. Maria, L. Q. Flagg, A. Savva, J. Surgailis, B. D. Paulsen, D. Moia, X. Chen, S. Griggs, J. T. Mefford, R. B. Rashid, A. Marks, S. Inal, D. S. Ginger, A. Giovannitti and J. Nelson, *Journal of the American Chemical Society*, 2021, **143**, 14795-14805.
31. D. A. Koutsouras, L. V. Lingstedt, K. Lieberth, J. Reinholz, V. Mailänder, P. W. M. Blom and P. Gkoupidenis, *Advanced Healthcare Materials*, 2019, **8**, 1901215.

32. A. Wang, D. Jung, J. Park, G. Junek and H. Wang, *IEEE Transactions on NanoBioscience*, 2019, **18**, 248-252.